SLAC-PUB-111
May 1965

EXPERIMENTAL TECHNIQUES*

W.K.H. Panofsky
Stanford Linear Accelerator, Stanford University, Stanford, California

In most general terms the techniques of experimental high energy physics are intermediate between two extremes: those methods in which essentially all events initiated in a primary of secondary target are registered in the apparatus, and those in which selectivity is involved before primary data are recorded. Approximating the first category are the track chambers which will form the subject of another talk at this conference. As to the items in the second category I shall restrict myself to two: (a) magnetic spectrometers, and (b) selection of photon energies. It is perhaps appropriate that these two topics be emphasized in a conference devoted to high-energy electromagnetic interactions. In such interactions usually only a very small fraction of the events occurring are "of interest" in the experiment; the great bulk of events are low-momentum transfer, purely electromagnetic events which, at least in principle, do not contain new information. Hence "pre-selection" is of greater importance in this area than in the other branches of high-energy physics.

(Paper to be delivered at International Symposium on Electron and Photon Interactions at High Energies, DESY, June 8-12, 1965.)

*Work supported by U.S. Atomic Energy Commission.

Spectrometers used in high energy physics were generally developed initially by scaling and adapting the single lens, point-to-point focusing devices of low-energy nuclear physics. However, as energies enter the multi-BeV range, this scaling process loses validity. The reasons are: (1) Momentum resolution must be matched by angular resolution to correspond to a consistent value of center-of-mass energy resolution. Algebracally this requires an angular resolution δ_θ related to the fractional momentum resolution δ_p given by $\delta_\theta = \delta_p \left\{ \text{Tan} \frac{\theta}{2} + \frac{M}{E_1 \sin\theta} \right\}$, where E_1 is the incident energy, M is the rest energy of the target nucleon, and θ is the laboratory scattering angle; the first term dominates at high energies and intermediate angles. (2) Liquid hydrogen and deuterium targets are used for almost all experiments; therefore long target lengths must be used. As long as the target length is less than 0.02 to 0.04 radiation lengths, internal radiative effects will predominate over radiation straggling in the target. (3) Single lens spectrometers of high performance become very massive. For these reasons the spectrometer described here represent a convergence of the principles of the momentum analysers of low energy nuclear physics and the beam transport systems of high energy physics.

What I might call a "pure" spectrometer will transform a given pair (θ, p) of the kinematic variables at the production point into a single resolution element. (Figure 1.) On the other extreme we might consider a hodoscope arrangement determining a coordinate X_o preceeding a magnet bending the central particle orbit through an angle α at a radius of curvative ρ, followed by two hodoscopes separated by a drift distance L. (Figure 2.) The linear transfer matrices give the expression for $\Delta\theta$ and Δp shown on Fig. 2, assuming θ and X to be in a single plane; here

Δp and $\Delta\theta$ are the deviations in momentum and production angle from the central setting. Calculations based on this type of geometry places extremely severe limits on the multiple scattering permitted in the hodoscopes if a resolution δp in the 0.1% range is required. Moreover, at least for poor duty cycle linear accelerates, the accidental rate would be prohibitive for most processes.

Naturally a whole continuum of arrangements ranging from a "pure" spectrometer to a pure "hodoscope" arrangement combined with a bending magnet of arbitrary focusing property are possible.

As example of the "pure" spectrometer we will here consider primarily "line-to-point" focusing spectrometers for use with high energy electrons and photons which disperse θ and p at right angles; for mechanical reasons θ is dispersed horizontally and p vertically. In principle the same objective can also be met by a mixed system using point-to-point focusing both in the vertical and horizontal plane; the production angle θ can then be retrieved by an additional plane of hodoscopes following the focal plane. A coincidence between counter arrays at these two foci is thus required, with consequent higher accidental background rate when "structure" in the center-of-mass system is to be observed above a continuum. This alternative generally seems to offer little advantage over the "pure" spectrometer, but may be simpler mechanically. In this class, is a version of the "Schrägfenster" spectrometer of DESY[1] in which $\Delta\theta$ is measured at an intermediate focus and a linear combination of $\Delta\theta$ and Δp is observed at a secondary focus.

An example of a "pure" spectrometer located in a horizontal plane is the rotated quadrupole spectrometer,[2] described previously. In this instrument θ is first focused in a horizontal plane, but this focal position is imaged into a vertical coordinate through a "mixing" quadrupole. This system has been analyzed in detail to second order in all input co-ordinates but the complexity of alignment and of other adjustments made it less attractive than the other alternative systems which I will describe.

At high energies we are thus led to consider the family of multiple element spectrometers dispersing momentum vertically but providing line-to-point focus horizontally. At SLAC two such instruments are being designed; Table I gives a comparative table of parameters. In order to ascertain that the angular and momentum resolutions meet requirements, we have to be concerned with both first and second order optics. First order optics enters only to determine the momentum resolution δ_p: the dispersion must be sufficiently large so that the vertical magnification times the target height does not exceed the momentum resolution interval. This condition fixes in essence the required total size of the bending magnet, or more precisely the total available bending magnetic flux. In second order the situation is more complicated. If we consider the total initial variables $(X,\theta,y,\varphi,z,\delta_p)_o$ then following the formalism developed by K.L. Brown,[3] we can write an aberration matrix for each magnetic unit of the spectrometer composed of "geometric" matrix elements such as $(X_{final}|X_o^2)$, $(X_{final}|X_o\theta_o)$ etc. and including also "chromatic" terms $(X_{final}|\theta_o\delta_p)$, $(X_{final}|X_o\delta_p)$ and the like. We can then combine the resultant second order transfer matrices from each magnetic component and thus arrive at a program for obtaining both first and second order optics for the complete compound

system. The spectrometers in question were designed by using such a program, using essentially a trial and error procedure, guided by certain insight into the second-order effects. The resultant system for the 8 GeV instrument was configured as shown in Fig. 3. A physical picture of the instrument is shown in Fig. 4. Figure 5 shows the "thin lens" equivalent of the instrument, showing how the vertical point-to-point and horizontal line-to-point focussing is achieved. The resultant actual orbits are shown in Fig. 6. The system was optimized for maximum solid angle meeting the resolution requirements of Table I. Table II shows the overall transfer matrix (angles in milliradians; distances in cm). We note that the desirable dispersion characteristics listed in Table I are approximately met. To minimize 2nd order coefficients, certain general properties are helpful: (1) to reduce chromatic aberrations in the vertical plane, the focusing orbits originating from a line target should have minimum slope during the bending magnet. This is indeed satisfied here, since the angle between the "sine-like" focussing orbit and the symmetry axis as shown in Fig. 6 can actually be chosen to be near zero. (2) Aberration terms like $(y|\varphi_o\delta_p)$ correspond actually to a tilt in the focal plane through an angle ψ_y given by $-\tan\psi_y = (y|\delta_p)\,(\varphi|\varphi_o)\big/(y|\varphi_o\delta_p)$. If we tilt the focal plane about a horizontal axis so that its plane is at 15° to the central ray, then the overall effect on the final coordinates is given by Table III. Since from the first order optics (Table II) a 0.1% momentum excursion gives a vertical spread of 0.3 cm, and a 0.3 mrad angular spread a horizontal excursion of 1.34 cm, we see that the resolution requirements are met. The result of these calculations has been verified at DESY by direct orbit tracing.

The solution for the 8 BeV spectrometer was developed at the expense of the dispersed beam slanting upward. As the energy becomes larger this results in progressively more serious technical problems. For this reason the dispersion for the 20 GeV instrument was achieved by two bends of opposite sign, but with the vertical focusing orbits designed to make the dispersion of each magnet additive. The dispersed beam thus emerges horizontally.

Figure 7 shows the lay-out of components and Fig. 8 the geometrical configuration of the 20 GeV instrument. The "double bend," required to produce a horizontal emergent beam was achieved at some sacrifice, but also produces some advantages. It can be shown[4] that the tangent of the angle between the final focal plane and the central ray of a high energy instrument using quadrupoles and uniform field bending magnets only is proportional to $(N + 1)^{-1}$ where N is the number of cross-overs in the dispersion plane. Hence the focal plane "tilt" angle for this instrument would be too small unless corrected by appropriate sextupole elements. Figure 9 shows the "thin lens" equivalent of the "S-bend" instrument and Fig. 10 shows the resultant orbits as actually computed. Table IV gives the first order transfer matrices of the instrument and Table V gives the final X and y coordinates in the focal plane as a function of both 1st and 2nd order terms. It is seen that all the specified resolutions appear to be met for the full aperture. An advantage of the double-bend instrument is that we have an intermediate focus in the dispersion plane as can be seen in Fig. 10. Hence we can place an intermediate slit near the symmetry plane of the instrument, thereby decreasing the flux of pole-scattered particles reaching the detector.

Several detectors are appropriate to instruments of this kind, depending on the experiment to be performed. Optimum utilization of data and minimum rates of accidental coincidences would indicate a two dimensional array (Fly's eye) set of counters. Although such an arrangement is not excluded, the number of required elements (about 2000 for the 8 GeV instrument) would involve both very high costs and excessive mechanical complications if scintillators are used. A compromise is to use two grids of scintillators at right angles in a coincidence matrix. Accidental coincidences at any one (θ,p) "bin" are then always accompanied by a coincidence elsewhere, and can thus be rejected by computer logic, unless the rates are too high. Another principle would be to use only a one-dimensional set of counters oriented in the (θ,p) plane to correspond to a given excitation energy in the center-of-mass frame. This arrangement is particularily suitable for small angle inelastic electron scattering and small angle photo-production studies. In all these cases the basic detection grid in the focal plane must be followed by a particle identification system; I will not discuss alternate designs of such systems here. Suffice it to say that at large angles to the beam particle discrimination will pose severe problems if electrons are to be observed, since the expected pion to electron rates are extremely high.

Since spectrometers have a selective function -- i.e., since they reject all but a small fraction of the pheonomena occurring in a target -- data reduction essentially concurrent to the experiment is needed to monitor the experiments. This need, in combination with the multiplicity of data channels and of the magnetic elements involved makes the use of an on-line computer highly desirable.

My second topic deals with the experimental methods of photon selection. Considerable progress in this field has been made since the last conference and I would like to mention some points of particular interest.

High-energy photo-reactions are usually produced in a Bremsstrahlung beam filtered through a low-Z absorber to reduce the low-energy photon component. Four methods have been proposed or are under study to further "monochromatize" the photon beam. These are:

(a) The use of "tagged photons" -- i.e., observing the photo-induced process in coincidence with a recoil electron from the radiator.

(b) The use of photons produced by Compton scattering of photons in a laser beam from a high-energy electron beam.

(c) The use of photons radiated from a monochrystal bombarded by high-energy electrons.

(d) The use of photons from annihilation of energetic positrons in flight.

The use of "tagged" photons is an old idea but is limited in application due to the problem of the low data rates required to avoid accidental coincidences.

The idea is originally due to Koch at Illinois and Camac at Cornell. It was used extensively first by McDaniel and collaborators.[5]

Pine and others have recently "tagged" photos at the California Institute of Technology to obtain calibration sources for counters and other low counting rate applications. Drickey at SLAC has shown that even at a poor duty cycle a beam useful for spark chamber events can be obtained. E.g., for a typical arrangement an event rate of 2500 per hour can be obtained for a 100 μbarn cross section at an accidental coincidence background of 25%.

Experiments using "tagged" photons for total cross section measurements of photons are in progress at CEA.[6]

The method of Compton scattering of laser photons has been proposed both in Armenia[7] and in the U.S.[8] Both groups calculated possible intensities, energy spectra and polarizations which might be obtained. Table VI indicates typical values computed by Milburn. There is little hope that this method can lead to photon beams of monochromaticity sufficient such that the primary energy would be a useful kinematic constraint in the analysis of a photon induced event; at best it can be hoped that the background of unwanted photons be reduced. A further problem in the application of the method is that the available photon energy is only a fairly small fraction of the electron energy, unless intensive laser sources in the very short optical wavelengths can be developed.

Recently the Tufts University - CEA group[9] has observed the expected process successfully. Photons of 0.85 GeV were produced by scattering of the 6943 Å quanta from a ruby laser on the 6 GeV electron beam. The laser beam is reflected by a mirror to form a light beam in the direction opposite to the circulating electron beam of CEA. The back-scattered photons were observed in a Cerenkov Counter. The experiment at this time is mainly an "existence proof" rather than the source of a useful beam. The experiment has shown that the intensity of the back-scattered light was proportional to the product of the electron beam and laser beam intensities. The actual number of photons was probably 15-20 for each 0.2 joule of laser incident pulse.

The scattering of laser light by fast electrons has also been observed in the USSR;[10] the laser photons were scattered on a 600 MeV beam, resulting in 7 MeV back-scattered photons. The principal motive of experiments of this kind is not as much their intrinsic interest, since these processes

make very low four-momentum transfer, but their potential application to beam formation. Milburn has studied practical installations, as have the Armenian workers. Milburn calculates a photon output for a feasible geometry at SLAC of 3×10^4 photons per laser joule per 1 μsec pulse of the accelerator; the number could be increased by an order of magnitude for 0.1 μsec pulses if the pulse timing precision can be achieved. Thus the laser beam is equivalent to about 10^{-8} radiation length of radiator in the electron beam; residual gas background can therefore become appreciable, but can be controlled. Useful intensities are thus possible, but the question of achieving useful monochromatization is quite difficult. The characteristic angle ($\gamma^{-1}_{\text{effective}}$) defining the angular variation of photon energy k with angle θ in the equation $(k/k_{max}) = 1/[1 + (\gamma_{eff}\theta)^2]$ is given by $\gamma_{eff} = \gamma/[1 + 4\,(\gamma k_i/mc^2)]^{\frac{1}{2}}$ where k_i is the laser photon energy; for 20 BeV electrons $\gamma^{-1}_{eff} = 3 \times 10^{-5}$ radians; monochromatization to 1% thus requires control of the angle between the electron beam and the outgoing photon to 3×10^{-6} radians. Even at SLAC this is a formidable problem; it is likely that monochromatization for reducing background can be achieved, but that a line width sufficiently narrow to produce a constraint in the analysis of track chamber events is exceedingly difficult. Thus possibly the most promising application of laser beam photons is based on their high polarization rather than their spectrum. However, much effort is clearly required to reduce this technique to practice.

It has been pointed out by Mozley and de Wire[12] that the intensity peaks observed in the bremsstrahlung spectrum produced by electrons on monochrystals could be used as a possible candidate for a monochromatic source. The beautiful experiments by Diambrini and co-workers[13] demonstrated that the

spectrum radiated by 1 GeV electron on a single diamond crystal had the theoretically predicted "sawtooth" shape. Mozley and de Wire pointed out that the "sawtooth" shape could be converted into a series of peaks by restricting the angular tolerance between the incident electron beam and the outgoing photon beam to angles of order γ^{-1}. We are here thus again forced to angles in the 10^{-6} radian range and thus to very large distances and constraints on incident electron phase space. Hence the problems of practical realization are not dissimilar to those involving laser beams. However, a radiation length of 10^{-4} can be used without excessive multiple scattering and thus higher intensities are feasible than with laser beams. The enhancement observed by Diambrini, et. al., should increase rapidly with energy, provided we make the dubious assumption that the calculations based on Born approximation remain valid. In diamond the beam heating effects may force operation at less than maximum incident electron beam. However, recently a group of Japanese workers[14] have obtained energy peaks from single Silicon crystals similar to those obtained earlier in diamond by Diambrini and co-workers (Fig. 11). The measurements were made with incident electrons of 720 MeV; therefore the enhancement is less than that observed by the Italian group. Nevertheless, Kato et. al. were able to demonstrate the sharpening of the intensity dependence on the angle between the incident beam and the crystal axes as the collimation of the outgoing photons was tightened. As the result of the successful observation of the spectral fine structure of high energy bremsstrahlung from Silicon, it is probably worth while to re-open the question of using crystaline radiators in practical application. Nevertheless, the angular precision required and the incoherent background make this method not too attractive.

The radiation from monochrystals is highly polarized; such polarized bremsstrahlung has been used for photoproduction studies.[15] This method gives results in agreement with the earlier work on polarized beams from noncrystalline targets, but permits thicker radiators.

The method for photon beam monochromatization which looks most attractive for hydrogen bubble chambers is the use of annihilation of positrons in flight. The photon energy k observed at an angle θ from positrons of energy $\gamma\mu$ is given by $k/\mu = (1 + \gamma) / (1 + \gamma\,\theta^2/2)$. The angular distribution of the cross section per unit solid angle of the emitted photons varies as θ^{-2} for $\theta\gamma \gg 1$, while the cross section for the competing bremsstrahlung process varies as θ^{-4}. Hence the ratio of annihilation to bremsstrahlung can be reduced by increasing θ until the photon energy k decreases substantially below the incident energy; this occurs if $\theta \sim \gamma^{-\frac{1}{2}}$ according to the above equation.

The use of monochromatic photon beams by positron annihilation has been used extensively in low energy photo-nuclear reactions. Its use for high energy electrons was first discussed by Cassels.[16] Further, more detailed, calculations are due to Guiragossián.[17] The problem here is to choose parameters, in particular the photon angle, such that the ratio of photons in the peak to that in the continuum is acceptable without degenerating the energy excessively. Figure 12 shows a typical curve pertaining to such a compromise and the parameters pertaining to it. The accuracy of monochromatization is given by $dk/k = (k/\mu)\,\theta\,d\,\theta$. Hence the photon direction must be accurate to $\sim 10^{-4}$ rad for a 1% photon accuracy. Hence from this point of view this method is superior to the ones previously discussed. With the $\sim$ 1 μA of positrons expected at SLAC, intensities are amply sufficient for bubble chamber use.

There exists an interesting alternative in combining the beam tagging and monochromatization techniques.[18] The two γ-rays from positron annihilation will have a fixed geometrical relationship to one another. Therefore, if one γ-ray enters the bubble chamber, the other one can be located in a conventional spark chamber with lead plates. Spatial resolution should be adequate to determine which γ induced event in the bubble chamber corresponds to a matching photon in the spark chamber.

All these methods of monochromatizing real photons are, of course, in competition with the analysis of virtual photon processes induced by inelastic muon or electron scattering. I will not make such comparisons here; several authors, including L. Hand, D. Drickey, M. Perl, J. Tinlot and several others have analyzed possible future virtual photon experiments using track chamber techniques. At the risk of oversimplifying the description of a complex series of alternatives, I might summarize that the real photon techniques described above appear superior particularly if background problems are considered. However the analysis of inelastic events gives of course additional information such as on polarization dependence, on the contribution of longitudinal matrix elements and on the pertinent form factors.

REFERENCES

1. W. Kern and K.G. Steffen DESY/E 3,4,5 (1962). M.L. Hubner, private communication.
2. W.K.H. Panofsky, D. Coward, and Brown, "A High-Resolution 20 BeV Spectrometer Resolving Momentum and Production Angle Independently," Proceedings of the International Conference on High-Energy Physics, Dubna, 1964.
3. K. L. Brown, "First- and second-order aberration coefficients of wedge magnets," "The general first- and second-order theory of beam transport optics," "Part II: Reduction of the general first- and second-order theory to the case of the ideal wedge magnet," SLAC Internal Report, Stanford Linear Accelerator Center, Stanford University, Stanford, California (1963-1964).
4. K. L. Brown, private communication.
5. John W. Weil and Boyce D. McDaniel, Phys. Rev. 92, 391, 1953.
6. R. Wilson, private communication.
7. F. R. Arutynian et. al, Physics Letters, Vol. 4, Number 176 (1963) and Zh. Exsp. Theor. Fir. Vol. 45 No. 312, 1963 (JETP 18, 1964).
8. Richard H. Milburn, Physics Rev. Letters, Vol. 10, No. 75 (1963).
9. Bemparad, Milburn, Tanaka CEAL-1014; January 1965.
10. O. F. Kulikov, Y. Y. Telnov; E. I. Filippov, and M. N. Yakimento, Physical Letters 13, p. 344 (1964).
11. R. H. Milburn, SLAC Report, August 1964; in preparation.
12. R. F. Mozley, and J. De Wire, Nuovo Cimento 27, 1281 (1963).
13. G. Barbiellini, G. Bologna, G. Diambrini and G. P. Murtas, Phys. Review Letters 8, p. 112, (1962) and 8, p. 454, (1962).

14. S. Kato, T. Kifune, Y. Kimmura, M. Kobayaski, K. Kondo, T. Nishikawa, H. Sasaki, K. Takamatsu, S. Kikuta, and K. Kohra, Journal Phys. Soc. Japan 20, p. 303 (1965).

15. G. Barbiellini, G. Bologna, J. De Wire, G. Diambrini, G. P. Murtas, G. Selt, Supplements Nuovo Cimento 2, 4, p. 666, (1964).

16. J. Cassels, "Some aspects of target area design for the proposed Stanford two-mile linear electron accelerator," SLAC M Report, 1960.

17. Z.G.T. Guiragossian, "Almost monochromatic photon beams for a hydrogen bubble chamber, 1963," SLAC Internal Report, Stanford Linear Accelerator Center, Stanford University, Stanford, California, and J. Ballam and Z.G.T. Guiragossian, Proceedings of the International Conference on High-Energy Physics, DUBNA, August 5-15, 1964.

18. D. Drickey, "Tagged Photons," SLAC Internal Report, Stanford Linear Accelerator Center, Stanford University, Stanford, California (1965).

FIGURE CAPTIONS

1. "Pure" spectrometer.
2. "Pure" hodoscope.
3. Magnetic components of 8GeV/c spectrometer.
4. Pictorial view of 8 GeV/c spectrometer.
5. Thin lens equivalent of 8 GeV/c spectrometer.
6. Plots of computed orbits starting either with unit slope on the axis (sine-like orbit) or with zero slope at unit displacement (cosine-like orbit). The momentum dispersion of a ray starting along the central axis is also shown.
7. Magnetic components of 20 GeV/c spectrometer.
8. Pictorial view of 20 GeV/c spectrometer.
9. Thin lens equivalent of 20 GeV/c instrument.
10. Plot of computed orbits in 20 GeV/c spectrometer under the combination of initial conditions used in Fig. 6.
11. Plot of bremsstrahlung intensity by 720 MeV electrons incident on silicon as observed by Kato et al.[14]
12. Plot of the total ray spectrum produced by 15 GeV positrons in hydrogen observed at an angle of 11.92 milliradian.

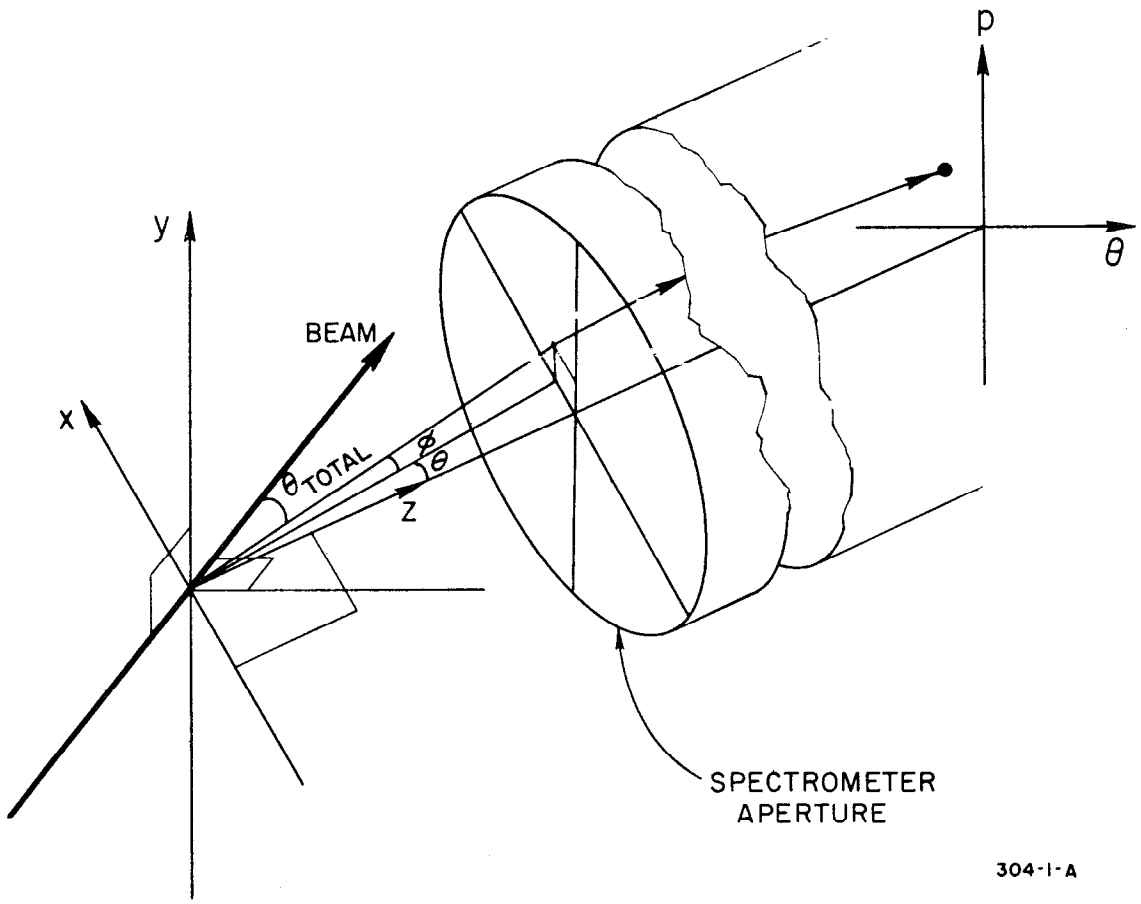

FIG.1 -- " PURE " SPECTROMETER

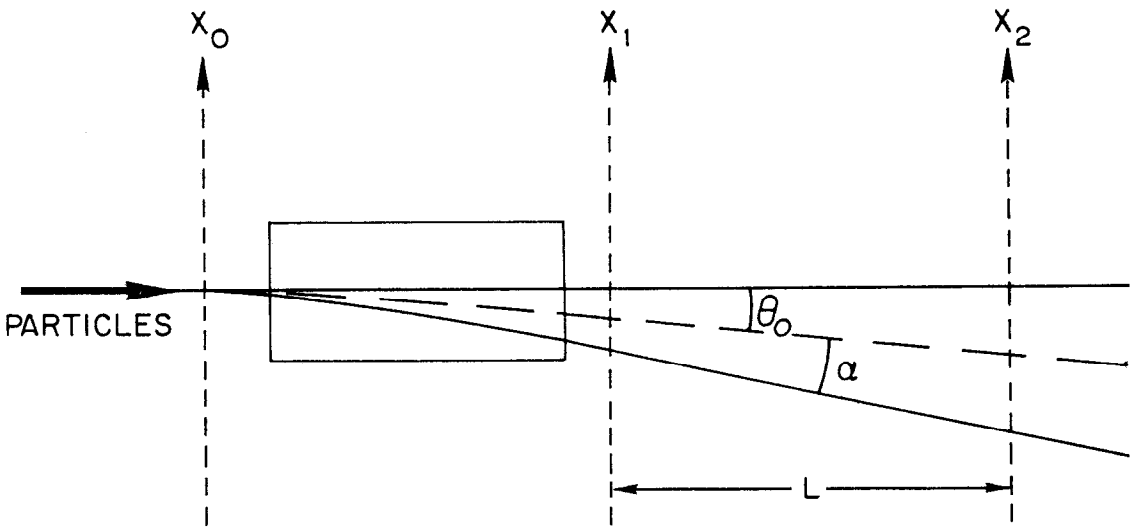

$$\delta_p = \frac{X_2 \sin\alpha - X_1 [\sin\alpha + (L/\rho)\cos\alpha] + X_0 (L/\rho)}{L(1-\cos\alpha)}$$

$$\theta = \frac{X_2 - X_1}{L} + \frac{X_1 - X_0}{\rho}\left(\frac{1-\cos\alpha}{\sin\alpha}\right)$$

304-2-A

FIG. 2--"Pure" hodoscope.

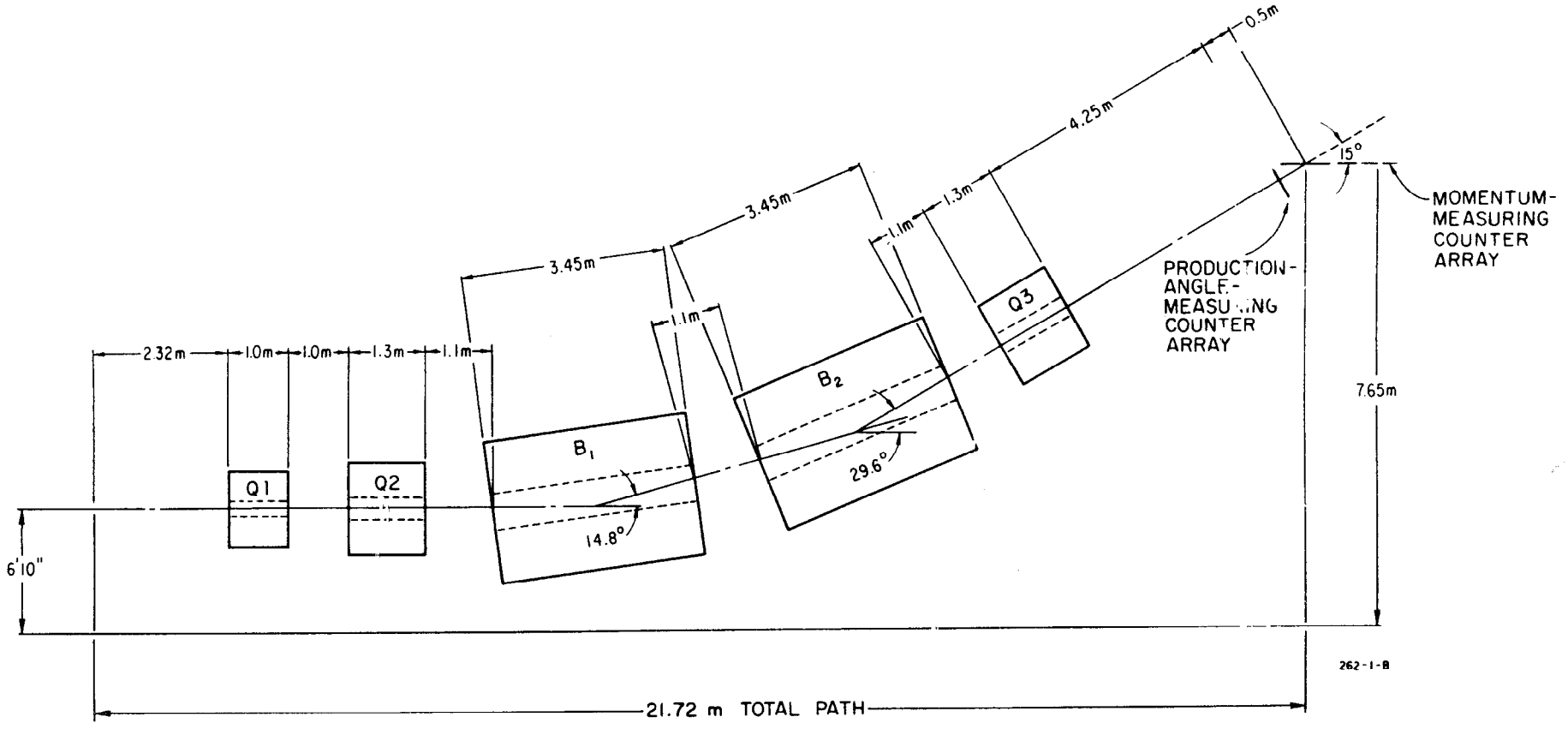

FIG. 3--Magnetic components of 8 GeV/c spectrometer.

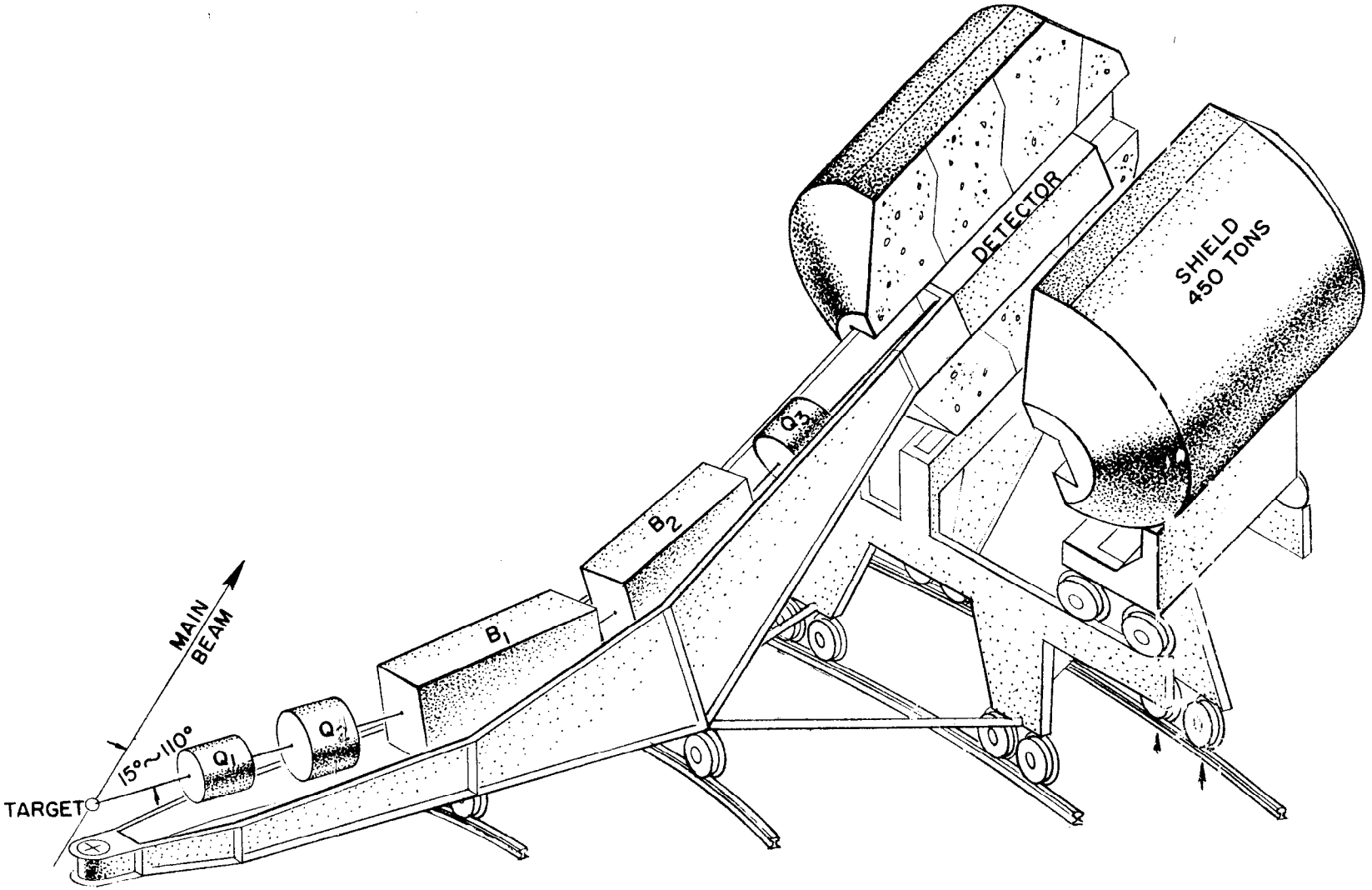

FIG. 4--Pictorial view of 8 GeV/c spectrometer.

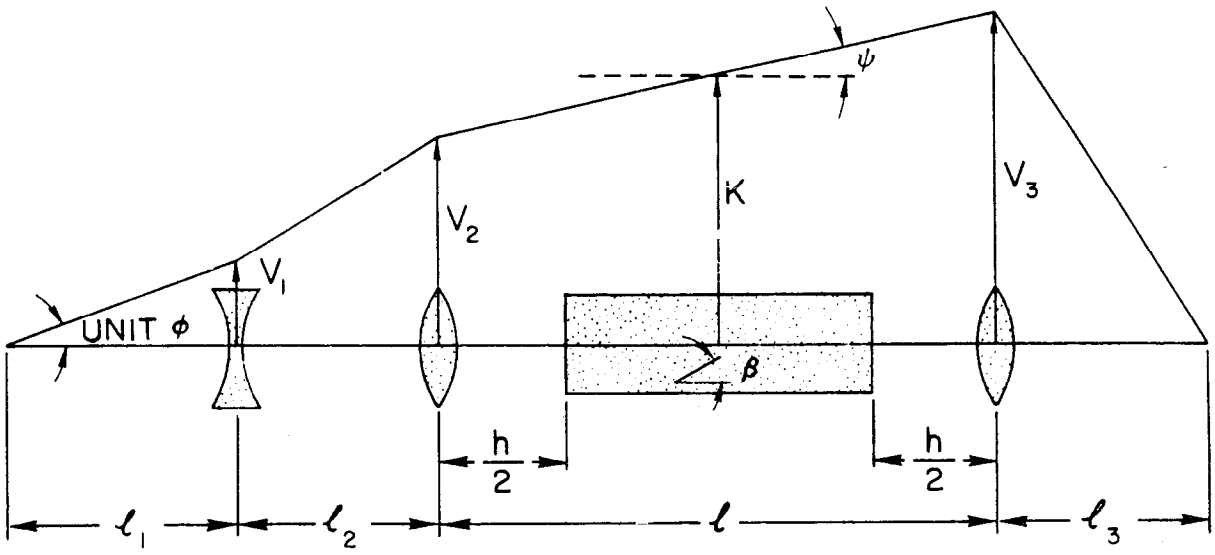

VERTICAL PLANE

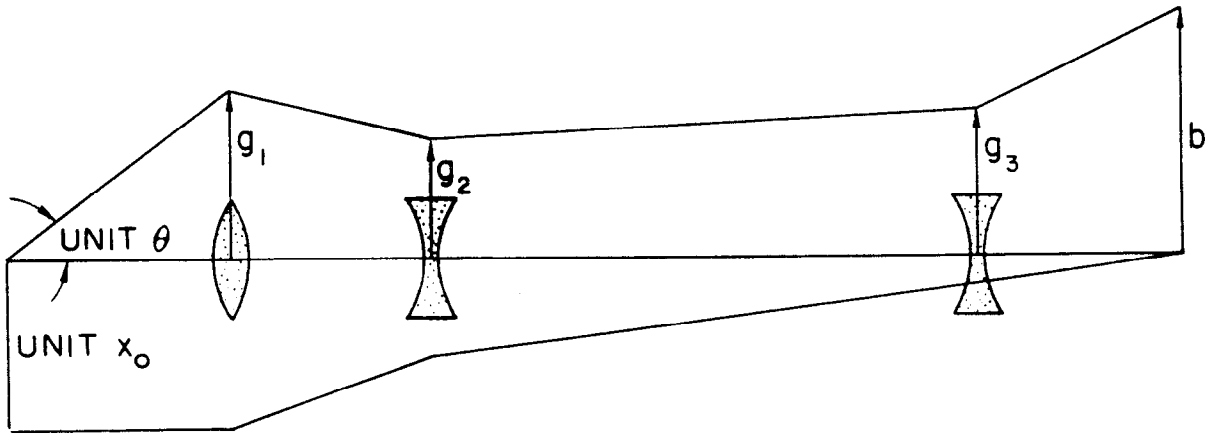

HORIZONTAL PLANE

262-2-A

FIG. 5--Thin lens equivalent of 8 GeV/c spectrometer.

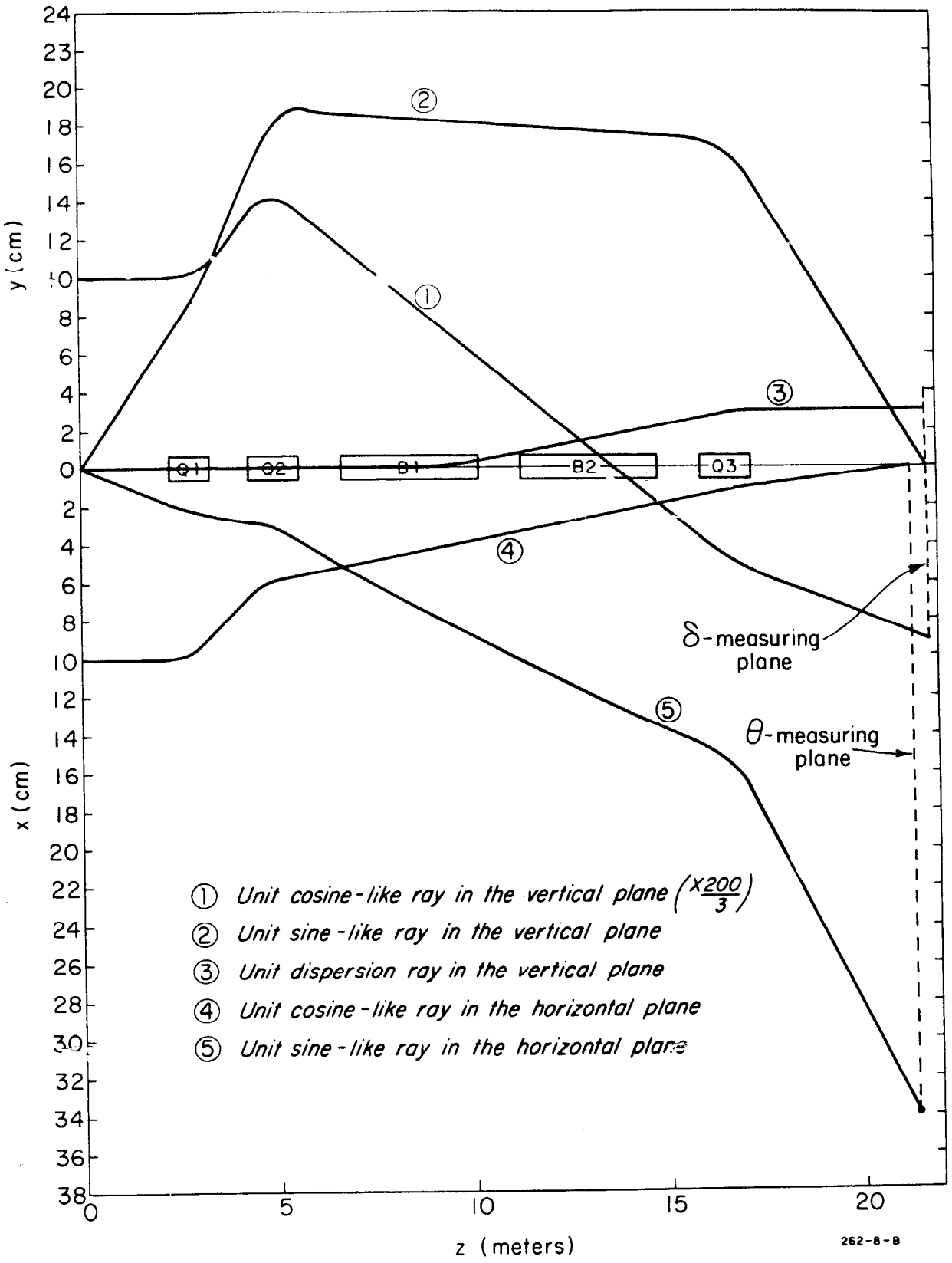

FIG. 6--Plots of computed orbits starting either with unit slope on the axis (sine-like orbit) or with zero slope at unit displacement (cosine-like orbit). The momentum dispersion of a ray starting along the central axis is also shown.

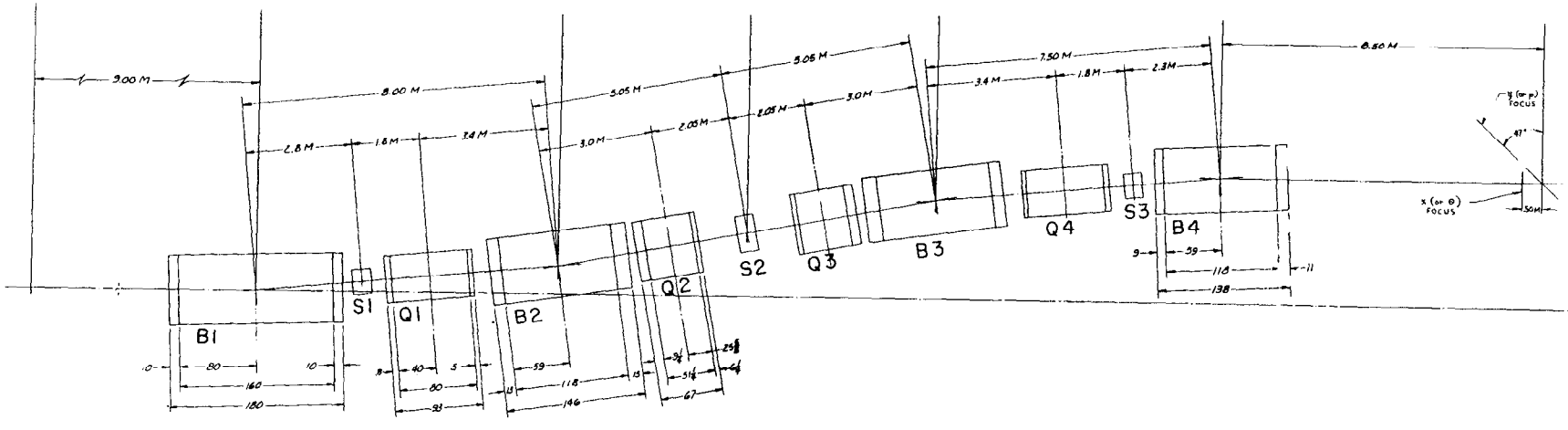

Fig. 7 – MAGNETIC COMPONENTS OF 20 GeV/c SPECTROMETER

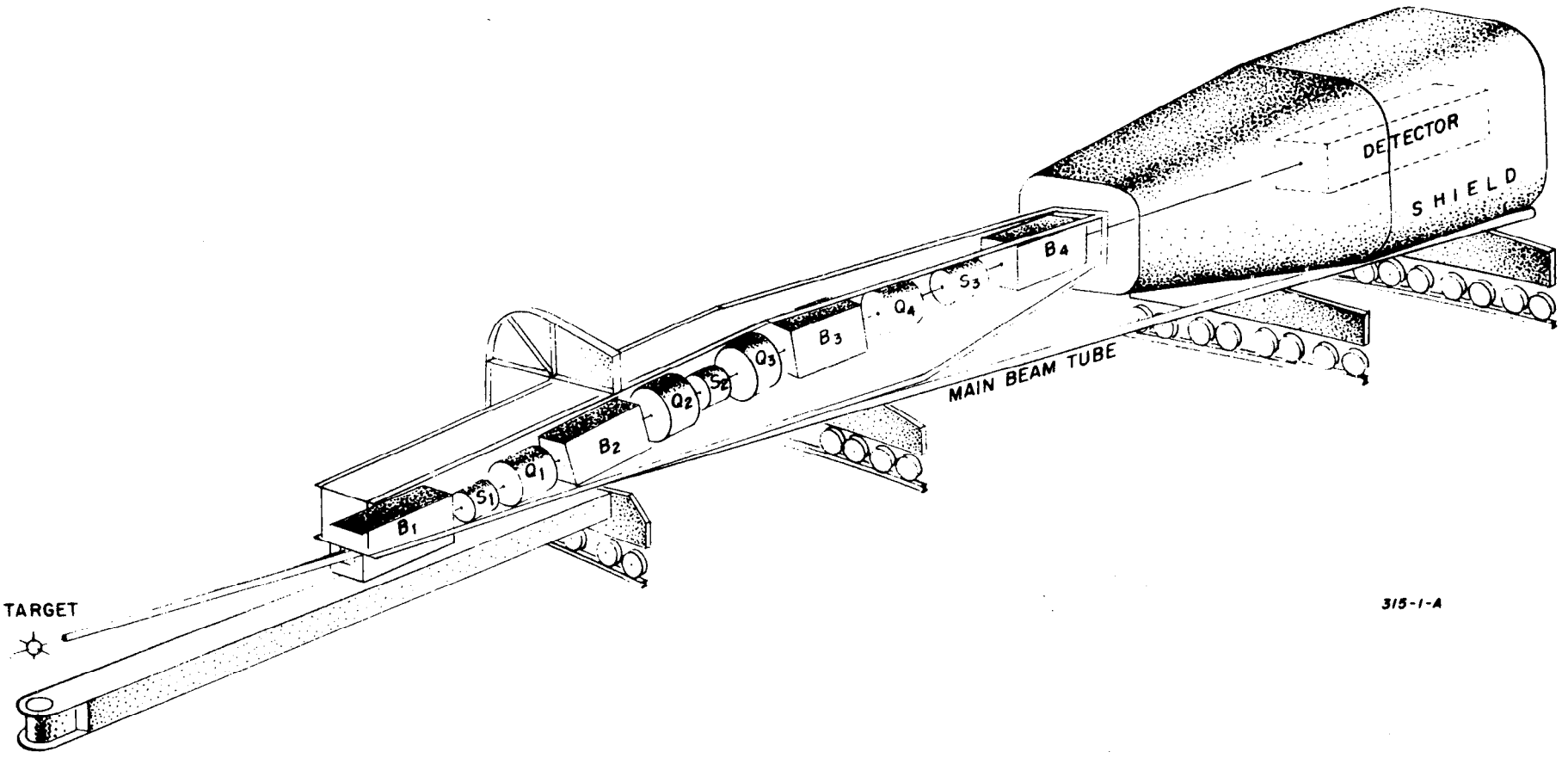

FIG. 8--Pictorial view of 20 GeV/c spectrometer.

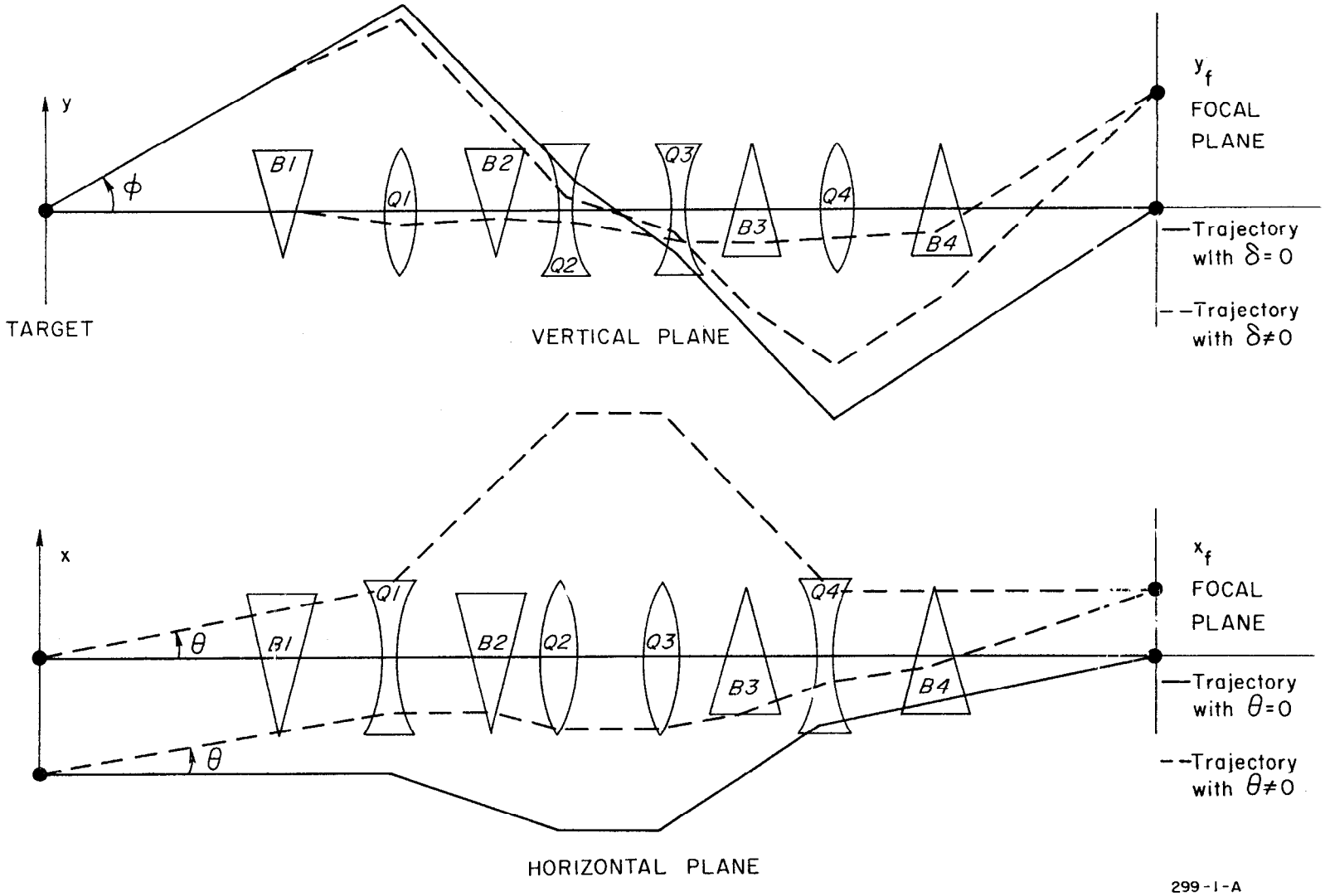

FIG. 9--Thin lens equivalent of 20 GeV/c instrument.

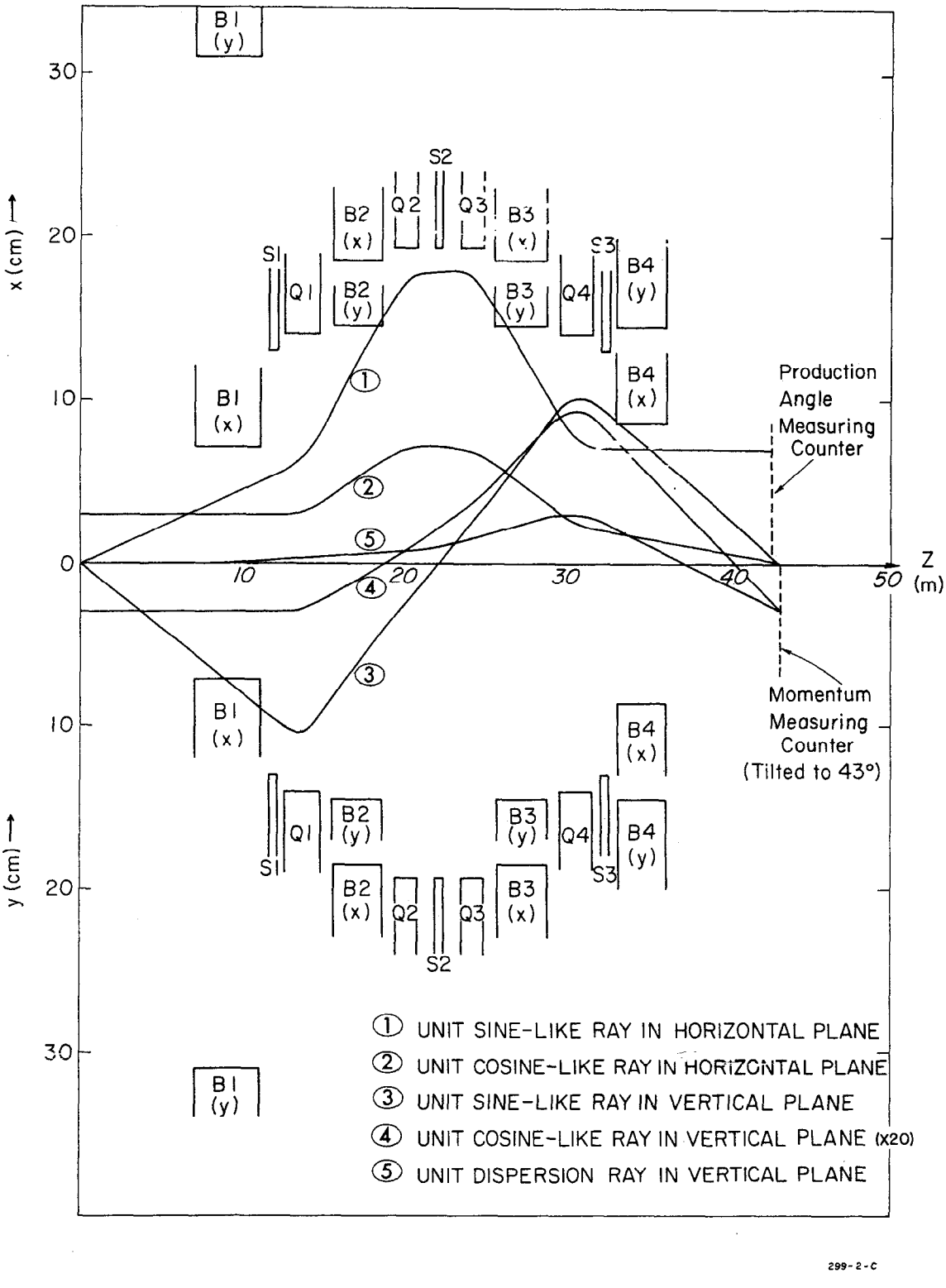

FIG. 10--Plot of computed orbits in 20 GeV/c spectrometer under the combination of initial conditions used in Fig. 6.

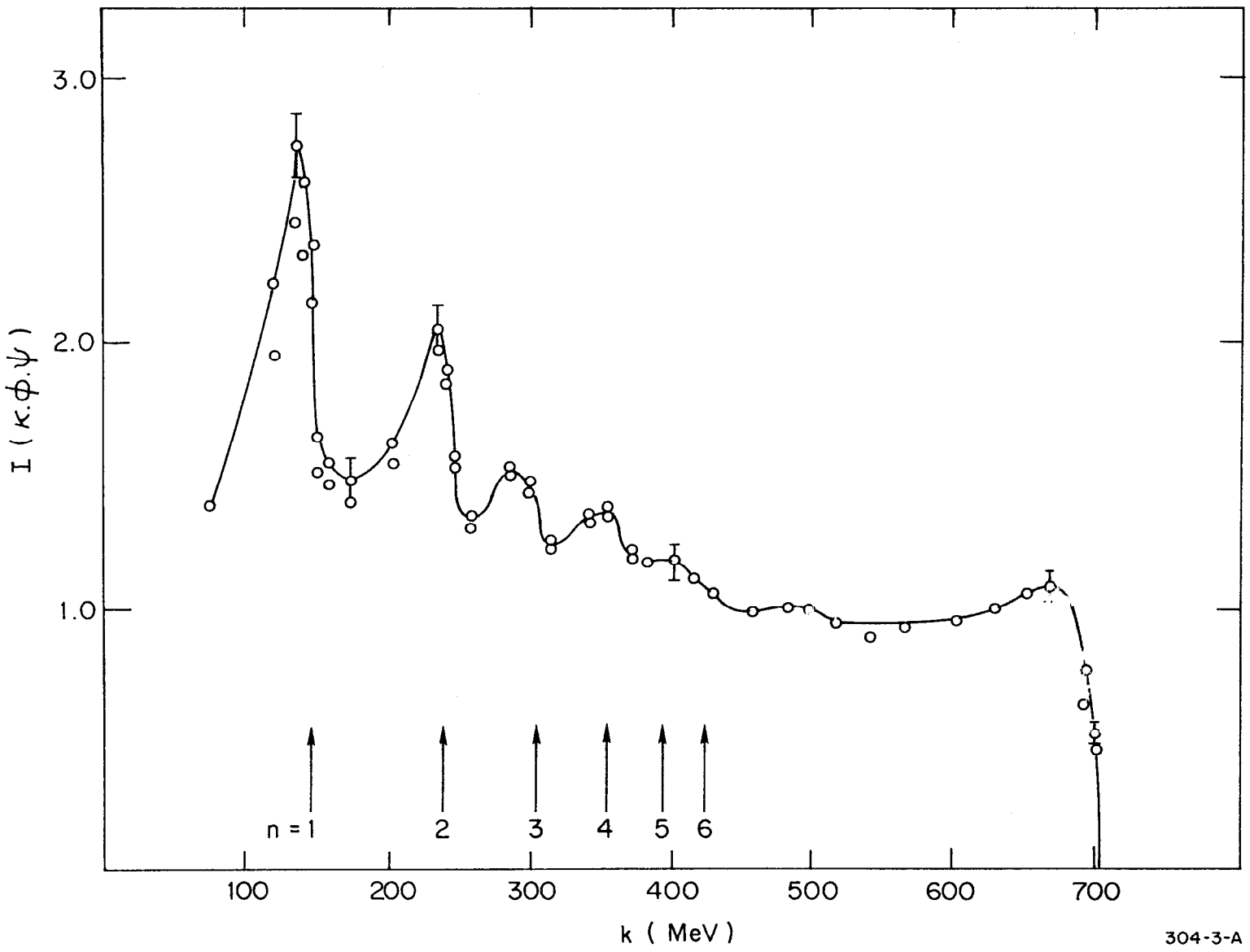

FIG. 11--Plot of bremsstrahlung intensity by 720 MeV electrons incident on silicon as observed by Kato et al.[14]

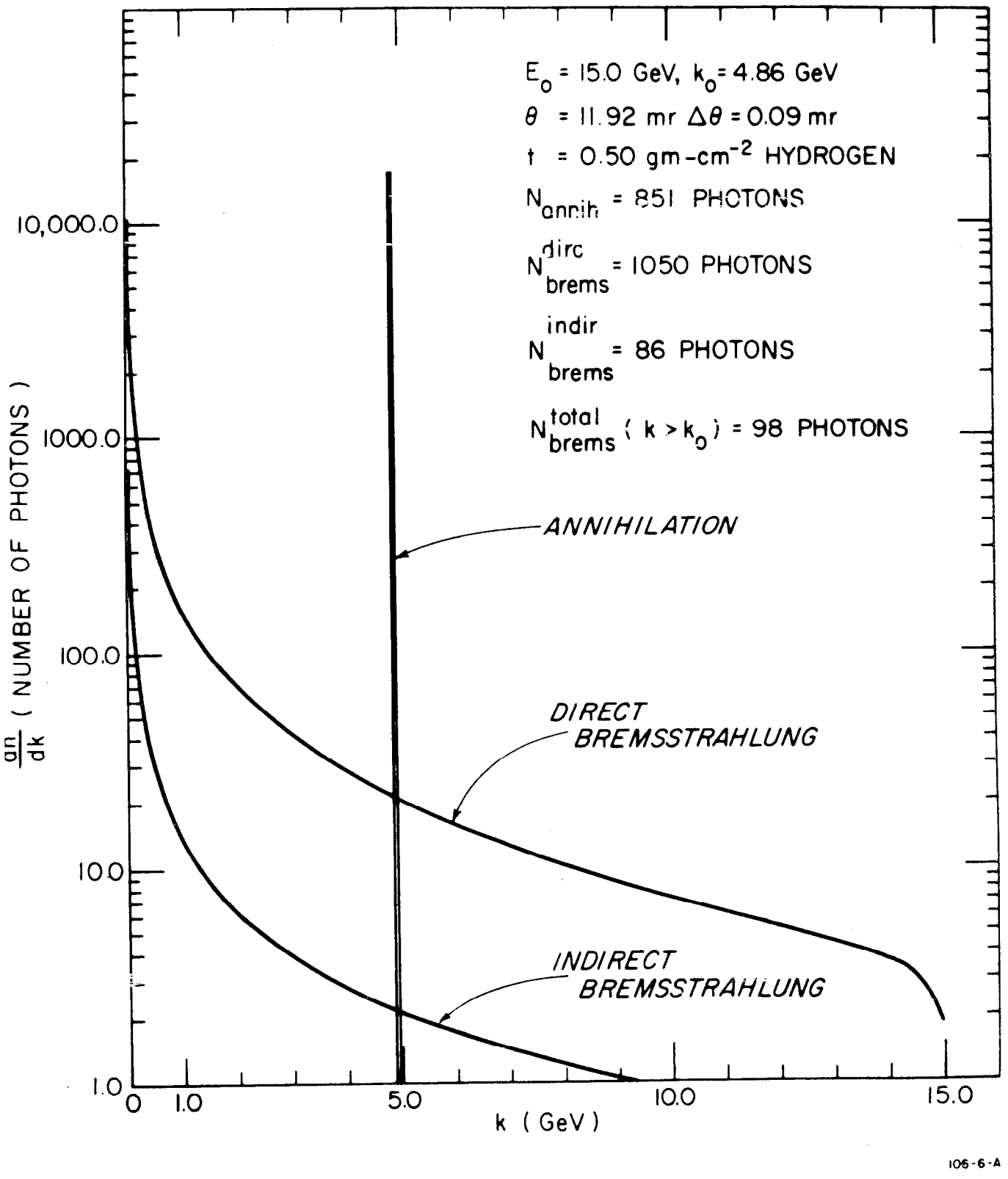

FIG. 12--Plot of the total γ ray spectrum produced by 15 GeV positrons in hydrogen observed at an angle of 11.92 milliradian.

TABLE I

SPECIFICATIONS OF THE SLAC 8 GEV/C AND 20 GEV/C SPECTROMETERS

Momentum (max)	20 GeV/c	8 GeV/c
Momentum resolution	± 0.05%	± 0.05%
Solid angle acceptance	10^{-4} ster.	10^{-3} ster.
Momentum acceptance	± 2%	± 2%
Angular resolution	0.3×10^{-3} rad	0.3×10^{-3} rad
Angular range (production angle)	$\pm 4.5 \times 10^{-3}$ rad	$\pm 8 \times 10^{-3}$ rad
Azimuthal angle	$\pm 8 \times 10^{-3}$ rad	$\pm 30 \times 10^{-3}$ rad
Maximum target length (projected)	3 cm	10 cm
Minimum angle at which beam will miss instrument	$\approx 3^{\circ}$	$\approx 12^{\circ}$

TABLE II-a

TRANSFER MATRIX FOR VERTICAL ORBITS OF 8 GEV/C INSTRUMENT

(Units: Length in cm, angle in mr, momentum in %)

	x_o	θ_o	y_o	Φ_o	z_o	δ_o
x	-0.12	4.477	0	0	0	0
θ	-0.236	4.741	0	0	0	0
y	0	0	-0.947	0	0	-2.955
Φ	0	0	-0.845	-1.056	0	0.041
z	0	0	0.253	0.312	1	-0.382
δ	0	0	0	0	0	1

TABLE II-b .

TRANSFER MATRIX FOR HORIZONTAL ORBIT OF 8 GEV/C INSTRUMENT

(Units: Length in cm, angle in mr, momentum in %)

	x_o	θ_o	y_o	Φ_o	z_o	δ_o
x	-0.000	4.240	0.000	-0.000	0.000	0.000
θ	-0.236	4.741	0.000	-0.000	0.000	0.000
y	-0.000	0.000	-0.905	0.053	0.000	-2.957
Φ	-0.000	-0.000	-0.845	-1.056	0.000	0.041
z	0.000	0.000	0.253	0.312	1.000	-0.382
δ	0.000	0.000	0.000	0.000	0.000	1.000

TABLE III

EQUATION GIVING THE VERTICAL AND HORIZONTAL OUTPUT COORDINATES IN TERMS OF ALL LINEAR AND ALL BI-LINEAR COMBINATIONS OF THE INPUT VARIABLES OF THE 8 GEV/C SPECTROMETER

$$x = [4.24\ \theta_o + 0.0108\ \theta_o \delta_o]$$

$+ 0.0405\ x_o \delta_o$	(± 0.81 cm)
$- 0.000688\ \theta_o \Phi_o$	(± 0.165 cm)
$+ 0.000177\ x_o \Phi_o$	(± 0.0531 cm)
$+ 0.000947\ x_o y_o$	(± 0.00142 cm)
$- 0.00053\ \theta_o y_o$	(± 0.000635 cm)

$$y = [- 2.955\ \delta_o + 0.00417\ \delta_o^2 + 0.000312\ \theta_o^2]$$

$- 0.947\ y_o$	(± 0.14 cm)
$+ 0.00126\ \Phi_o \delta_o$	(± 0.076 cm)
$- 0.00368\ y_o \Phi_o$	(± 0.017 cm)
$- 0.000154\ x_o \theta_o$	(± 0.012 cm)
$+ 0.0000197\ x_o^2$	(0.0020 cm)
$+ 0.0033\ y_o \delta_o$	(± 0.0017 cm)
$+ 1.08 \times 10^{-6}\ \Phi_o^2$	(0.00097 cm)
$- 0.00253\ y_o^2$	(-0.00006 cm)

TABLE IV-a

TRANSFER MATRIX FOR VERTICAL ORBITS OF 20 GEV/C INSTRUMENT

(Units: Length in cm, angle in mr, momentum in%)

	x_o	θ_o	y_o	φ_o	z_o	δ_o
x	0.033	1.531	0.000	0.000	0.000	0.000
θ	-0.652	-0.066	0.000	0.000	0.000	0.000
y	0.000	0.000	0.927	-0.000	0.000	2.826
Φ	0.000	0.000	3.410	1.078	0.000	5.061
z	0.000	0.000	0.495	0.305	1.000	0.291
δ	0.000	0.000	0.000	0.000	0.000	1.000

TABLE IV.b

TRANSFER MATRIX FOR HORIZONTAL ORBITS OF 20 GeV/c INSTRUMENT

(Units: Length in cm, angle in mr, momentum in %)

	x_o	θ_o	y_o	φ_o	z_o	δ_o
x	0.000	1.534	0.000	0.000	0.000	0.000
θ	-0.652	-0.066	0.000	0.000	0.000	0.000
y	0.000	0.000	0.757	-0.054	0.000	2.573
φ	0.000	0.000	3.410	1.078	0.000	5.061
z	0.000	0.000	0.495	0.305	1.000	0.291
δ	0.000	0.000	0.000	0.000	0.000	1.000

TABLE V

EQUATION GIVING OUTPUT COORDINATES CORRECT TO

SECOND ORDER IN THE INPUT VARIABLES FOR THE 20 GeV/c SPECTROMETER

$$x = [1.534\ \theta_o + 0.0177\ \theta_o\delta_o]$$

$$-0.0139\ x_o\ \varphi_o \quad (\pm 0.334 \text{ cm})$$

$$+0.0048\ \theta_o\ \varphi_o \quad (\pm 0.173 \text{ cm})$$

$$-0.105\ \theta_o\ y_o \quad (\pm 0.0708 \text{ cm})$$

$$-0.0878\ x_o\ y_o \quad (\pm 0.0395 \text{ cm})$$

$$-0.00254\ x_o\delta_o \quad (\pm 0.0153 \text{ cm})$$

$$y = [2.826\ \delta_o - 0.0421\ \delta_o^2 - 0.0167\ \theta_o^2]$$

$$+0.927\ y_o \quad (\pm 0.139 \text{ cm})$$

$$-0.000836\ \varphi_o^2 \quad (-0.0535 \text{ cm})$$

$$+0.0407\ y_o\varphi_o \quad (\pm 0.0488 \text{ cm})$$

$$-0.0029\ x_o\theta_o \quad (\pm 0.0391 \text{ cm})$$

$$+0.0042\ x_o^2 \quad (0.0378 \text{ cm})$$

$$+0.0291\ y_o\delta_o \quad (\pm 0.00873 \text{ cm})$$

$$+0.0653\ y_o^2 \quad (0.00147 \text{ cm})$$

$$+8.99 \times 10^{-5}\Phi_o\delta_o \quad (\pm 0.00144 \text{ cm})$$

TABLE VI

TABLE OF ENERGY AND POLARIZATION OF RUBY LASER PHOTONS
BACK-SCATTERED BY ELECTRONS OF INITIAL ENERGY E

Electron Energy E	Peak Output Photon Energy	Peak Polarization
1.02 GeV	28 Mev	1.00
2.92	216	1.00
4.16	426	0.99
4.60	515	0.99
5.11	628	0.99
5.48	715	0.99
5.84	806	0.99
6.21	903	0.99
6.57	1.00 GeV	0.99
8.76	1.69	0.98
11.69	2.83	0.96
20.80	7.55	0.91
41.60	22.10	0.77
58.40	35.90	0.67